



10-2-6

NONLINEAR SEISMIC RESPONSE OF CABLE-STAYED BRIDGES SUBJECTED TO NONSYNCHRONOUS SUPPORT MOTIONS

Ahmed M. ABDEL-GHAFFAR¹ and Aly S. NAZMY²

¹Department of Civil Engineering, University of Southern California,
Los Angeles, California 90089-0242, USA

²Department of Civil Engineering, Polytechnic University, Brooklyn,
New York 11201, USA

SUMMARY

Nonlinear seismic-response characteristics of three-dimensional long-span cable-stayed bridges are studied. The cases of multiple-support as well as uniform seismic excitations of these long and flexible structures are considered. Three sources of nonlinearity are included in the analysis: cable-sag effect, axial force and bending moment interaction, and changes of geometry of the whole bridge due to its large deformations. A tangent stiffness iterative procedure as well as a step-by-step integration procedure are utilized in the analysis to capture the nonlinear seismic response. Numerical examples are presented to shed some light on the salient features of the seismic analysis of these contemporary and increasingly popular bridges.

INTRODUCTION

The future trend in the design of cable-stayed bridge structures, with longer center or effective spans, makes the need for nonlinear analysis inevitable. Since the nonlinearity in the behavior of this special type of flexible, long-span bridge is of geometric type, and mainly due to large deformations, it is essential to point out that when the center-span length increases, which will result in a considerable increase in the displacements and deformations of the bridge under strong ground shaking, a pronounced nonlinearity in the response may be expected. Furthermore, although for the present range of center spans (up to 1600 ft or 500 m), linear dynamic analysis is adequate, nonlinear static analysis under dead loads is still essential to start the linear dynamic analysis from the dead load deformed state (Fig. 1).

In this study, a general step-by-step integration technique is presented for the evaluation of the seismic response of geometrically nonlinear cable-stayed bridges. The structure is discretized in space into finite elements, mainly beam-column elements and cable elements, and the Wilson- θ Method [3] is used for the time discretization, to assure numerical stability of the algorithm for all time increments

Equations of Motion To separate the vibrational response from the quasi-static response in order to examine the dynamic or inertial as well as the kinematic effects, the equations of motion of the bridge can be written in the partitioned form:

$$\begin{bmatrix} M_{ss} & M_{sg} \\ M_{gs} & M_{gg} \end{bmatrix} \begin{Bmatrix} \ddot{y}_s \\ \ddot{y}_g \end{Bmatrix} + \begin{bmatrix} C_{ss} & C_{sg} \\ C_{gs} & C_{gg} \end{bmatrix} \begin{Bmatrix} \dot{y}_s \\ \dot{y}_g \end{Bmatrix} + \begin{bmatrix} K_{ss} & K_{sg} \\ K_{gs} & K_{gg} \end{bmatrix} \begin{Bmatrix} y_s \\ y_g \end{Bmatrix} = \begin{Bmatrix} 0 \\ 0 \end{Bmatrix}, \quad (1)$$

where $[M_{sg}]$, $[C_{sg}]$ and $[K_{sg}]$ are rectangular mass, damping, and stiffness matrices, respectively, of order $N \times g$ (where N = number of degrees of freedom of the finite element model and g = number of earthquake inputs). These rectangular matrices represent the coupling between the structural nodes not connected to the ground, and the support displacements due to seismic motion y_s is the total displacement of the structural nodes and y_g is the displacement of nodes connected to the ground. The mass and damping matrices are assumed to be constant, while the stiffness matrix is changing as a function of nodal displacements. Assuming that the displacements can be decomposed into quasi-static and vibrational displacements

$$\begin{Bmatrix} y_s \\ y_g \end{Bmatrix} = \begin{Bmatrix} y_{vs} \\ 0 \end{Bmatrix} + \begin{Bmatrix} y_{ps} \\ y_{pg} \end{Bmatrix}. \quad (2)$$

The elastic force computed in the above equation as $[K_{ss}](\{y_{vs}\} + \{y_{ps}\})$ can be viewed as the sum of two parts, vibrational elastic force (due to vibrational displacements), and pseudo-static elastic force (due to support displacement); see Fig. 2 This yields:

$$[K_{ss}(y_{vs} + y_{ps})]\{y_{vs}\} + \{y_{ps}\} = [K_{ss1}]\{y_{vs}\} + [K_{ss2}]\{y_{ps}\}. \quad (3)$$

For an unloaded structure with a static condition of support displacements the equilibrium is expressed by

$$[K_{ss2}]\{y_{ps}\} + [K_{sg}]\{y_{ps}\} = 0. \quad (4)$$

It should be mentioned that the stiffness matrix (whether the secant stiffness used in the equation of dynamic equilibrium, or the tangent stiffness used in the incremental equations of motion) is a function of the dead-load displacement plus the vibrational displacement (Fig. 2). Thus, the quasi-static displacement is not included in computing the stiffness. In the above, $\{y_{pg}\}$ is the vector of ground displacements at the supports of the structure. Substitution from Eqs. 2, 3 and 4 into Eq. 1 yields

$$[M_{ss}]\{\ddot{y}_{vs}\} + [C_{ss}]\{\dot{y}_{vs}\} + [K_{ss1}]\{y_{vs}\} = \{P(t)\}, \quad (5)$$

where

$$\begin{aligned} \{P(t)\} = & ([M_{ss}] [K_{ss2}]^{-1}[K_{sg}] - [M_{sg}])\{\ddot{y}_{pg}\} \\ & + ([C_{ss}][K_{ss2}]^{-1}[K_{sg}] - [C_{sg}])\{\dot{y}_{pg}\}. \end{aligned} \quad (6)$$

Generally, the contribution due to the damping term in the above equation is neglected; also, if a lumped mass idealization is used, $[M_{sg}]$ becomes a null matrix, in which case Eq. 6 reduces to

$$\{P(t)\} = [M_{ss}][K_{ss2}]^{-1}[K_{sg}]\{y_{pg}\} = -[M_{ss}][G_{ps}]\{\ddot{y}_{pg}\} \quad (7)$$

where $[G_{ps}]$ is the matrix of quasi-static functions, whose columns represent the static displacements corresponding to unit displacement of the supporting points. It can be assumed that these quasi-static functions (Fig. 3) remain constant during the earthquake-response excitation, and that they are not affected in shape by the change in the stiffness of the structure. Such an assumption is possible since the changes in $[K_{SS2}]^{-1}$ and $[K_{SG}]$ can cancel each other when they are multiplied, and since these quasi-static functions are normalized functions, whose maximum values equal to unity. The above assumption makes it possible to avoid inverting the stiffness matrix $[K_{SS2}]$ at the beginning of each iteration cycle, and thus saves a considerable amount of computational time.

Incremental Form of the Equations of Motion The equations of dynamic equilibrium at time t_i can be written in a matrix form. At a later time τ , where $\tau = \theta\Delta t$, the equations of dynamic equilibrium can also be written. Subtracting the first set from the second set of equations results in the incremental equations of motion:

$$[M]\{\hat{\Delta}y_i''\} + [C]\{\hat{\Delta}\dot{y}_i\} + [K_T(y_i)]\{\hat{\Delta}y_i\} = \{\hat{\Delta}P_i\} + \{P_i\} - [M]\{\dot{y}_i''\} - [C]\{\dot{y}_i\} - \{F_i^e\}. \quad (8)$$

In the above equation, the hat over Δ indicates that the increments are associated with the extended time step $\tau = \theta\Delta t$; $[K_T(y_i)]$ is the tangent stiffness matrix which is a function of the nodal displacements at time t_i , and is assumed to remain constant during the increment of time τ ; $\{y(t_i)\}$ and $\{P(t_i)\}$ are the vectors of dynamic nodal displacement and externally applied dynamic nodal forces at time t_i , respectively.

The Elastic Force Vector $\{F_i^e\}$ It is possible to calculate the elastic force vector $\{F_i^e\}$ by simply adding up the incremental force changes $\{\Delta F^e\}$; (Fig. 4-a). However, because the stiffness matrix $[K_T]$ is, in general, only an approximation, significant errors can accumulate in this procedure. Therefore, it is preferable to compute $\{F_i^e\}$ from the dead-load (D.L.) displacements plus the vibrational displacements at time t_i as follows (Fig. 4-b):

$$\{F_i^e\} = [K_S(y_{D.L.} + y_i)](\{y_{D.L.}\} + \{y_i\}) - \{F_{D.L.}^e\}, \quad (9)$$

in which $[K_S(y_{D.L.} + y_i)]$ is the secant stiffness based on the joint displacements and member forces due to both D.L. and vibrational displacements.

This process is usually carried out on the element level, where the member-end actions are computed for each element based on the D.L. and vibrational displacements using the secant stiffness of the element at this particular deformed state. Then, for each node, these internal forces are assembled and projected on the system global coordinates, for all the elements jointing at this particular node. By inverting the sign of these assembled forces for all the nodes, and subtracting from them the externally applied dead-load forces at the joints, the elastic force vector due to dynamic displacements, $\{F_i^e\}$, is obtained.

The Tangent Stiffness Matrix $[K_T(y_i)]$ The tangent stiffness matrix at any time t_i is assembled from the individual element tangent stiffness matrices at the same instant of time. For each element, its tangent stiffness $[k_T]$ is the sum of the elastic stiffness and the geometric stiffness $[K_T]$ changes as a function of both the nodal displacements and the member axial thrust. It is computed once at the beginning of each time step and used during iterations in this time step until convergence is achieved to some acceptable tolerance. This means that the modified Newton-Raphson technique is used in the iterative procedure to achieve equilibrium (to some tolerance) at the end of each time step.

THE USE OF MODAL SUPERPOSITION IN SOLVING THE NONLINEAR DYNAMIC PROBLEM

The solution of Eq. 8 for nonlinear systems, using a direct step-by-step integration procedure, requires the iterative solution of a nonlinear system of algebraic equations, equal in order to the number of degrees of freedom in the finite-element model. This may require the solution of a very large order system. Therefore, the modal response method is utilized to replace the original system of equations for the structure nodal displacements by a smaller system of equations for a system of generalized coordinates. In principle, the use of modal superposition simply involves a coordinate transformation, where the normal mode shapes serve as a set of orthogonal bases, from the finite element real displacement coordinates to the modal coordinates; the modal transformation is given by

$$\{y_i\} = [\Phi]\{q_i\} \quad , \quad (10)$$

where $[\Phi]$ are the mode shapes obtained using the tangent stiffness matrix in the dead-load deformed state, and $\{q\}$ is the vector of "nonlinear" generalized displacement.

Application and Validation Since the modes used here are those obtained using the tangent stiffness matrix of the bridge in the dead load deformed state, and are assumed to remain constant for the purpose of coordinate transformation during the entire earthquake analysis, the results obtained by this method need to be verified. Poor agreement was obtained between the results of this method and those of the direct integration method, when only 10 modes were used. In the current analysis 30 modes, which proved to be sufficient, are used for the purpose of coordinate transformation; these modes cover a band of the bridge vibration. Two models are considered in this study; the first model (I) has a center span of 1100 ft (335.5 m) and side spans of 480 ft (146.4 m) while the second model has a center span of 2200 ft (671 m) and side spans of 960 ft (292.8 m). The second model (II) represents the future trend in cable-stayed bridge design. Some of the ground motion records taken from the Imperial Valley (El Centro), California, earthquake ($M_L = 6.6$) of October 15, 1979 are employed in this study to define the multiple-input or non-synchronous motions as well as uniform support motions [2]. A damping ratio of 2 percent was assumed for all modes. Comparison between the results of linear and nonlinear dynamic analysis, following a nonlinear (as well as a linear) dead-load static analysis are presented in Figs. 5, 6 and 7.

Since the difference between linear- and nonlinear-dynamic analyses for Model I is small (Fig. 5), it is important to examine the validity of using linear static analysis and to investigate the necessity of performing a nonlinear analysis under dead loads to start the dynamic analysis (with the tangent stiffness at the dead-load deformed state). By examining Fig. 5, it is evident that there is not much difference between the results of the linear- and nonlinear-dynamic analyses for this 1100 ft center-span model. It is evident from Figs. 5, 6 and 7 that the nonlinear dynamic behavior of model II is more pronounced than in the case of Model I. Furthermore, there is a frequency shift observed in the response time-history; this is due to the fact that the overall stiffness of the bridge increases by the increase in the dynamic displacements as well as the forces. This result is consistent with the fact that the nonlinearity is of geometric type, and that it is mainly due to large deformations and an increase in the center-span length.

CONCLUDING REMARKS

1. Although for the present range of center of effective spans (up to 1600 ft or 500 m), linear dynamic analysis is adequate, nonlinear static analysis under dead loads is still essential to start the linear dynamic analysis from the dead load deformed state (Fig. 5).
2. For the recent and future trends of longer center span (≥ 2000 ft or 600 m), geometrically nonlinear dynamic analysis is necessary for computing the response of the bridge subjected to strong ground shaking (Figs. 6,7). Such trends make the need for such nonlinear analysis inevitable; this is essential not only for evaluating the stresses and deformations induced by environmental loads, such as vehicular traffic, wind, and earthquakes, but also for assuring safety during construction.
3. Multiple-support seismic excitations can have a significant effect and should be considered in the earthquake-response analysis of such long and complex three-dimensional structures; this effect is more pronounced when the structural redundancy gets higher (Figs. 6 and 7).

ACKNOWLEDGEMENT

This research is supported by the U.S. National Science Foundation (Grant No. CES-8717252) with Dr. S. C. Liu as the Program Director; this support is greatly appreciated.

REFERENCES

1. Fleming, J. F. and Egeseli, E. A., "Dynamic Behavior of a Cable-Stayed Bridge," Int. J. of Earthquake Engrg. and Struct. Dyn., Vol. 8, pp. 1-16, 1980.
2. Nazmy, Aly S. and Abdel-Ghaffar, Ahmed M., "Seismic Response Analysis of Cable-Stayed Bridges Subjected to Uniform and Multiple-Support Excitations," Report No. 87-SM-1, Dept. of Civil Eng., Princeton Univ., May 1987.
3. Wilson, E. L., Garhoomand, I., and Bathe, K. J., "Nonlinear Dynamic Analysis of Complex Structures," Int. Journal of Earthquake Engrg. and Struct. Dyn., Vol. 1, No. 3, 1973, pp. 241-252.

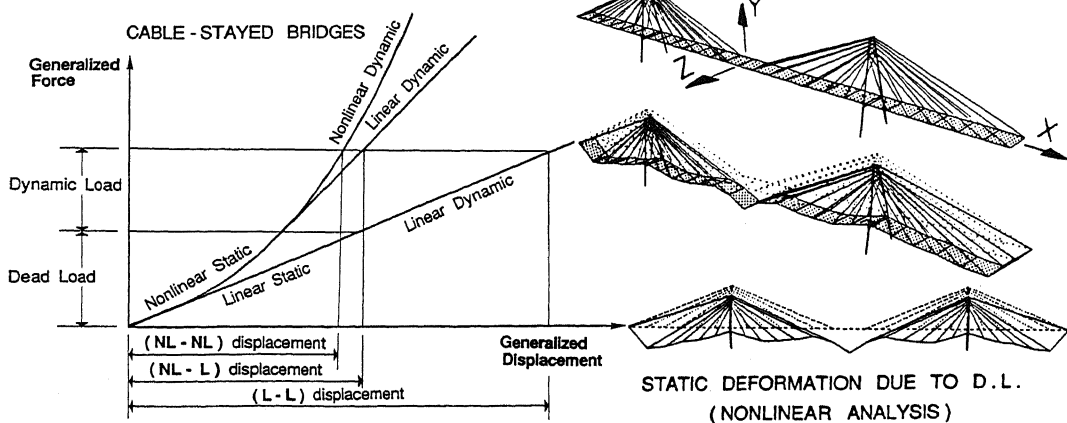
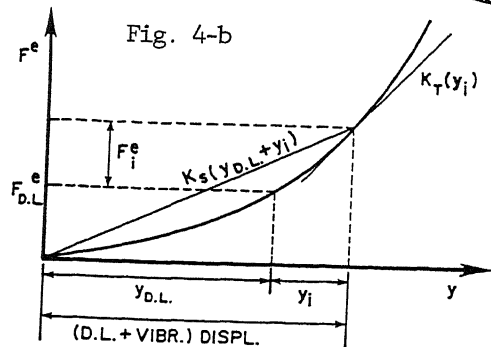
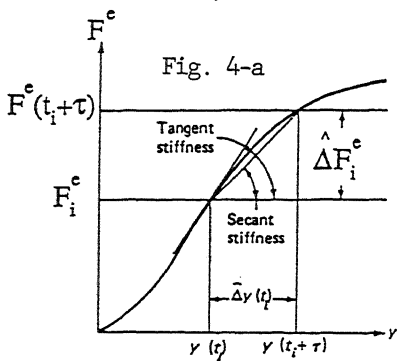
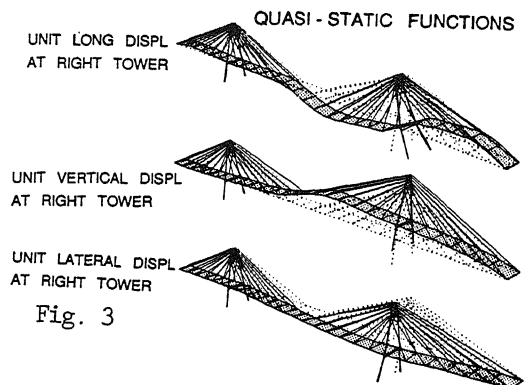
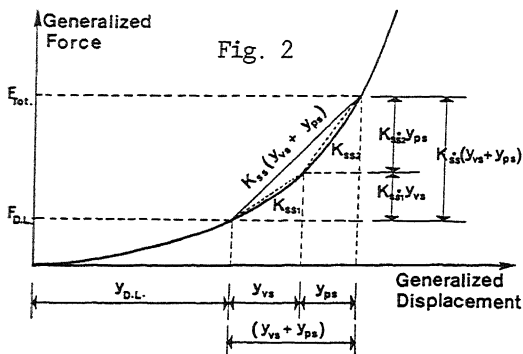


Fig. 1 Linear and nonlinear analyses (static and dynamic) of cable-stayed bridges.



3-D CABLE-STAYED BRIDGE - MODEL 1 - SPAN 1100 FT
UNIFORM EARTHQUAKE INPUT

3-D CABLE-STAYED BRIDGE - MODEL 2 - SPAN 2200 FT
MULTIPLE EARTHQUAKE INPUTS

